An Explanation of Higher Heat Transfer Efficiency in Laminar Structured Boundary Layers Than in Turbulent Boundary Layers

L. Momayez[1, 2], G. Delacourt[1], P. Dupont[1, 3], H. Peerhossaini[1], J. T. C. Liu[1, 4]

[1]Laboratoire de Thermocinétique -CNRS UMR 6607, École Polytechnique de l'Université de Nantes, BP 50609,44306, Nantes, France
[2]KhorramshahrUniverity of Marine Sciences and Technology, Khorramshahr, PB 669, 64199-43175, Iran
[3]LGCGM, EA3913, INSA de Rennes, Campus Beaulieu, 35043 Rennes cedex, France
[4]Division of Engineering and Center for Fluid Mechanics, Brown University, Providence, RI 02912-9104, USA
Ladan.Momayez@univ-nantes.fr

Résumé - Les études théoriques du développement spatial de tourbillons longitudinaux de Görtler stables montrent que, dans la région de développement non linéaire où les lignes isothermes ne sont plus sinusoïdales, le transfert de chaleur local associé à un « downwash » est très élevé et n'est que partiellement atténué par le faible transfert associé aux « upwash ». Toutefois, ces tourbillons longitudinaux, de la même manière que les tourbillons de Taylor entre des cylindres rotatifs, sont sujets aux instabilités secondaires en mode variqueux et sinueux. La similitude entre les fluctuations de vitesse longitudinale et les variations de température pour un nombre de Prandtl unitaire permet d'expliquer comment un taux de transfert de chaleur surfacique en absence de turbulence dépasse celui de la couche limite turbulente local sur plaque plane. Les comparaisons entre ces résultats théoriques et nos résultats expérimentaux sont donnés pour accompagner cette explication particulière.

Nomenclature

X	Streamwise direction (m)	U_{pw}	potential wall velocity (m/s), $U_{pw} = \frac{U_n}{\frac{R}{H} ln\left(1-\frac{H}{R}\right)} = 0.88 U_n$
Y	Normal-to-the-wall direction (m)		
Z	Spanwise direction (m)		
u v w	The corresponding (X,Y,Z) velocity components	Re_x	Reynolds number based on length scale x, $Re_x = U_n x / \upsilon$
		Re_c	Critical value of Re_x
λ_z	Spanwise wavelength of Görtler vortex	G_θ	Görtler number $\frac{U_n \theta}{\upsilon}\sqrt{\frac{\theta}{R}}$
Pr	Prandtl number, $Pr = \upsilon / k$	φ_w	Wall heat flux ($w.m^{-2}$)
St	Local Stanton number $St = \varphi_w / \rho C_p U_{pw}(T_{wall} - T_\infty)$	θ	Boundary layer momentum thickness
		R	Wall radius of curvature
T_∞	Free-stream temperature (K)	T_w	Wall temperature (K)
U_n U_0	free-stream velocity (m/s)	ν	kinematic viscosity
		u, v, w	corresponding velocity components are, respectively which are all normalized by U_0;
δ_0	coordinates are normalized by a viscous length scale $\delta_0 = \sqrt{\nu X_0 / U_0}$,	$\vec{u}$	three-dimensional steady counter rotating vortex velocities in vector form with components u, v, w.

$\vec{u}'$	three-dimensional fluctuation velocities in vector form with components u', v', w'	$r_c = R/\delta_0$	dimensionless concave plate radius
θ	$\theta = (T - T_W)/(T_0 - T_W)$ dimensionless mean temperature	θ'	$\theta' = T'/(T_0 - T_W)$ the fluctuation temperature where the free stream condition is denoted by subscript 0 and that on the wall by subscript W

1. Introduction

Counter-rotating streamwise vortices in boundary layers are known to enhance the surface heat transfer rates as demonstrated by a class of winglet vortex generators [1,2]. However, such "internals" give rise to significant drag increase and pressure rise requirement: a two to one relative heat transfer enhancement incurs a four to one drag rise for the flow regimes studied [1,2]. In the Laboratoire de Thermocinétique, efforts are made to generate streamwise vortices via fluid dynamical means without internals, through the use of centrifugal instabilities of the laminar boundary layer flow over slightly concave surface. In this case, the relative heat transfer enhancement and drag rise is one to one, considerably reducing the drag rise penalties.

In this paper, we bring together for the first time a synthesis from experimental [3-9] and theoretical studies [10-16] to explain a main issue of heat transfer enhancement. That is, the development of local heat transfer rates, which follows the laminar value initially, can overshoot the local turbulent value for a significant streamwise distance even in the absence of turbulence in the boundary layer. Only those experimental and theoretical ideas which intersect are focused upon to explain this particular issue. There exist many other experimental issues which remain and these are subjects of further studies to be undertaken.

2. Experimental studies

The convective heat transfer on a concave wall is experimentally studied [3-9] through measurements of wall temperature as well as flow field observations. Flows considered consist of a laminar boundary layer which develops on a realistic thick leading edge, in the presence of upstream small amplitude perturbations. The comparison of the streamwise evolution of the Nusselt and Stanton numbers shows that this last parameter describes more precisely the three-dimensional flow development [7] . The Görtler number based on the local Blasius momentum thickness, G_θ allows a better correlation of the different stages of development of the Görtler instability. Experimental parameters are usually represented in the $G_\theta - \beta_\theta$ plane [17], where β_θ is the dimensionless spanwise vortex wavelength. For a particular experimental condition and fixed spanwise vortex wavelength, the vortex wavelength parameter $\Lambda_{\lambda_z} = \mathrm{Re}_{\lambda_z}\sqrt{\lambda_z/R}$ is the slope of a log plot in the $G_\theta \propto \theta^{3/2}$ vs. $\beta_\theta \propto \theta$ plane.

In Figure 1 we present a particular case of Stanton number development for $\Lambda_{\lambda_z} = 570$ and $1 < G_\theta < 10$, for which $U_n = 3m/s$. Measurements include the hotwire for the flow field and surface temperature measurements for heat transfer. Experimentally it is more suitable to heat the surface and measure the response wall temperature whereas in theory the wall temperature is specified and surface heat transfer rates are obtained as result of computations. In both cases the dimensionless Stanton number is obtained.

The various stages of flow in Figure 1 are labeled as O, A, B, C, and D and are described below:

- zone OA: this zone corresponds to the leading edge region and its junction with the concave part of the model. In this zone the local St approximately follows the laminar boundary layer value on a flat plate. The deviation of the first few points is due to flow acceleration at the leading edge.

- zone AB: heat transfer on the concave wall deviates gradually from the flat plate by the appearance of a "plateau" with roughly constant Stanton number. This heat-transfer intensification is related to the growth of the nonlinear steady Görtler vortices by the effect of centrifugal instability.
- zone BC: the Stanton number gradually reaches values close to or above turbulent boundary layer values on a flat plate. This rapid increase in heat transfer coefficient (St) is due to the nonlinear secondary instability of the Görtler vortices [18] (3D unsteady flow)

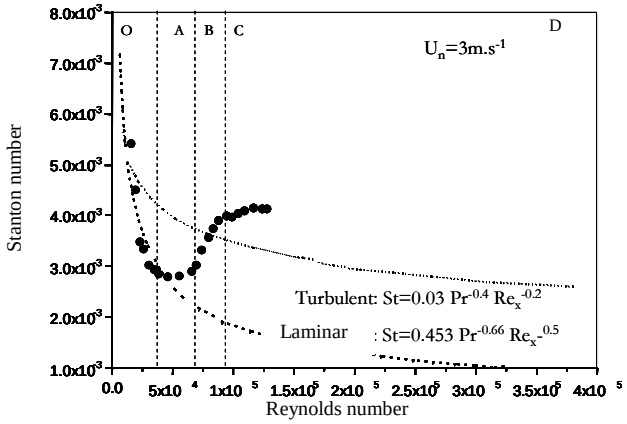

Figure 1 Evolution of Stanton number as a function of Reynolds number and freestream velocity 3 m/s ($\Lambda_{\lambda_z} = 570$).

- zone CD: heat transfer ceases to increase and follows the flat-plate turbulent curve. It has been observed [19, 20] that turbulent spots are present in the boundary layer at these Görtler numbers. The secondary instability induces large-scale coherent vortices in the flow that are more efficient for heat transport than the smaller turbulent scales.

Experimental measurements show that the spatial amplification of secondary instabilities, which are in the 38-45 Hz frequency range, is about 2 to 5 times that of the primary steady Görtler vortex. This "explosive" growth of the secondary instabilities is consistent with previous experiments[17]. The secondary instabilities can take the form of varicose mode as well as the sinuous mode [15-21]. A typical flow visualization [9,18]of the varicose mode in the XY plane is shown in Figure 2, and appears in the form of horseshoe vortices.

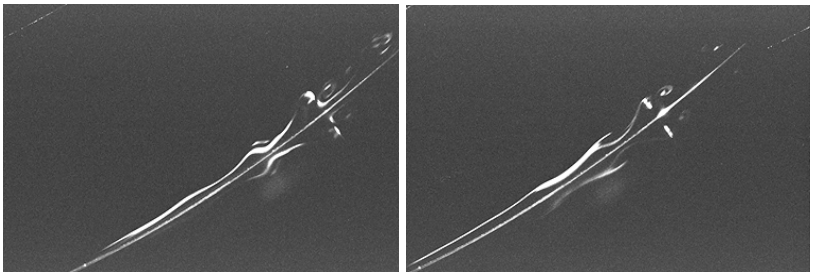

Figure 2: *Two visualizations of horseshoe vortices due to the varicose mode of secondary instability in plan (x-y) for a velocity Un=3m / s.*

This configuration is also confirmed by in-phase symmetrical hotwire responses positioned on both sides of the mean streamwise velocity "mushroom" structure in a downstream cross sectional plane in the "upwash" flow. In experiments where secondary instabilities are unforced, both modes (varicose and sinuous) coexists at about the same frequency.

Measurements of both the mean and fluctuation streamwise velocities are shown in Figure 3 for the case of natural, unforced development (where rms denotes the root mean square). Velocity profiles are shown in the XZ plane at various streamwise locations. The mean velocity develops from smooth to mushroom-like contours for iso-U lines and are more complex than the well shaped mushroom

structure from computations [11-14] . We notice that u_{rms} are located on both sides of the mushroom stem. It is learned from the contours that considerable coherent structures associated with secondary instabilities are present and that the significant rise of St in Figure 1 well above the local turbulent boundary layer value is accomplished by the transport effects of the coherent vortices rather than fully developed turbulence.

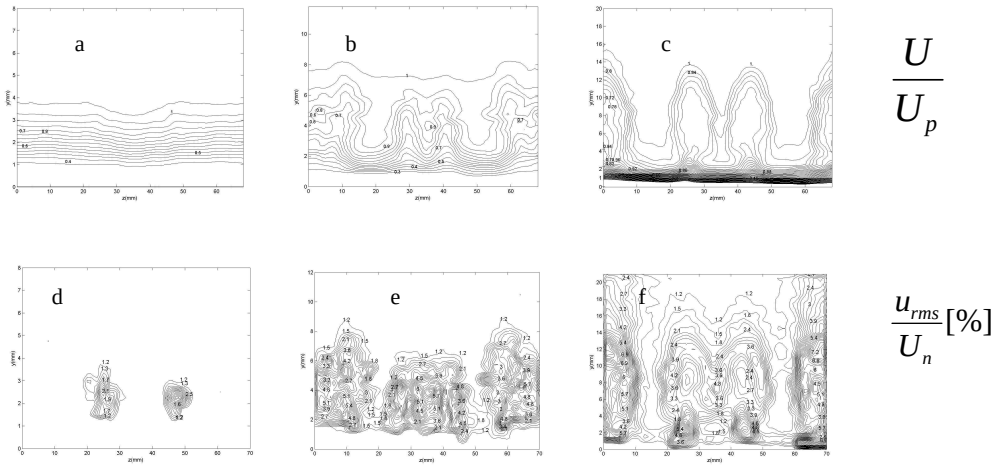

Figure 3. *Isocontour lines of* U/U_p , $u_{rms}/U_n[\%]$*(a) &(d) in X=15 cm (zone OA), (b) &(e) X=29cm (zone AB) (c) &(f) X=49cm (zone CD); iso-velocity contours plotted in the cross sectional YZ plane;* $U_n = 3\,\mathrm{m.s}^{-1}$.

3. Theoretical interpretations

The basis for understanding the behavior of surface heat transfer rates lies in the convective heat transfer description from thermodynamical considerations. From the assumption of an incompressible flow, the heat transport equation becomes uncoupled from that of momentum. The latter is in the present description, highly nonlinear and has been the subject of numerous studies [10-17]. The heat transport problem in the incompressible approximation is linear but is strongly dependent upon the convective velocities especially in the enhancement of heat transfer. We state the thermodynamical equations specific to the present problem after performing the Reynolds splitting. The vertical convective transport owing to secondary instabilities appear as if they are turbulent under the time average in the mean flow problem

$$\vec{u}.\nabla\theta = (\mathrm{Re}\,\mathrm{Pr})^{-1}\nabla_{yz}{}^2\theta - \nabla\cdot(\overline{\vec{u}'\theta'}) \tag{1}$$

The scaling which is reflected in the passive scalar transport (1) is imposed by the mean momentum problem. Similarly, the scaling from geometrically near-isotropic secondary instabilities is imposed on the scalar fluctuation transport

$$\theta'_t + u\theta'_x + v'\theta_y + w'\theta_z = +(\mathrm{Re}\,\mathrm{Pr})^{-1}\nabla^2\theta' + \nabla\cdot(\overline{\vec{u}'\theta'} - \vec{u}'\theta') \tag{2}$$

The boundary and upstream initial conditions for the mean flow are

$$y\to\infty:\theta=1,\quad y=0:\theta=0,\quad \theta(x,y,0)=\theta(x,y,\lambda_z),\quad \theta(x_0,y,z)=\theta_G$$

where θ_G is the upstream mean temperature consistent with the prevailing upstream Görtler vortex [11]. The boundary and upstream conditions for the temperature fluctuation are

$$y\to\infty:\quad \theta'=0,\quad y=0:\quad \theta'=0,\quad \theta'(x,y,0)=\theta'(x,y,\lambda_z),\quad \theta'(x_0,y,z)=\theta'_{\mathrm{lin}}$$

where θ'_{lin} is the upstream temperature fluctuation consistent with upstream secondary instabilities [16]. Considerable simplification of the thermodynamical problem is made through the recognition that an approximate Reynolds Analogy is possible for $\mathrm{Pr}=1$ between the mean and fluctuating temperature and the corresponding streamwise velocities of the nonlinear momentum problem

[14,15]. In this case, $\theta' = u'$, $\theta = u$, $-\overline{v'\theta'} = -\overline{v'u'}$; $St = C_f/2$. The Stanton number inferred from the nonlinear momentum problem[13] under the Reynolds analogy for $Pr = 1$ is shown in Figure 4. The conditions correspond to that of Swearingen & Blackwelder [21] for $\Lambda_{\lambda_z} = 462$.

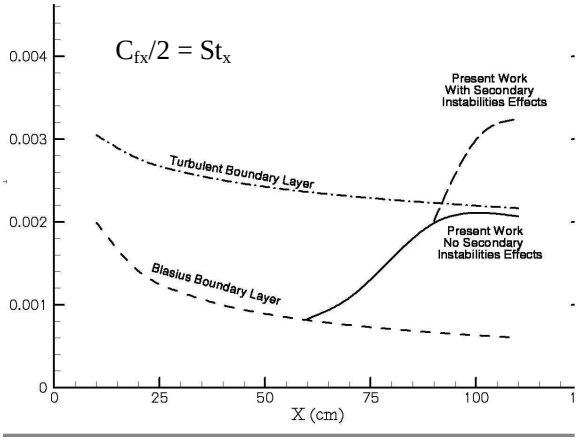

Figure 4. *Stanton number development for* $Pr = 1$*, inferred from the nonlinear momentum problem [13]*

In Swearingen & Blackwelder[21] the leading edge is sharp via suction along a spanwise strip immediately upstream. In this case, the complexities of a blunt leading edge is circumvented. The wall temperature is prescribed while the surface heat transfer rate is obtained from the solution of the problem, whereas in experiments it is convenient to heat the wall and obtain a response wall temperature. There are sufficient differences between conditions of the heat transfer computations and the conditions of Swearingen & Blackwelder[18] used here, so that it is more meaningful to have a side-by-side comparison for physical explanation rather than a less meaningful direct comparison. It is now understood that a bridging between laminar and turbulent boundary layer heat transfer can be made via the transport effects of steady streamwise vortices in the absence of secondary instabilities[10,12]. In order to explain the overshoot beyond the local turbulent value in the absence of turbulence, it is necessary to appeal to the effect of the "eddy heat flux" owing to the transport effects of the secondary instability. To this end, $-\overline{v'\theta'}$ is inferred from the local Reynolds stress $-\overline{v'u'} = -\overline{v'\theta'}$ of Yu & Liu [17] over a cross section. In general, regions of $-\overline{v'\theta'} > 0$ in the cross sectional plane dominate, especially after spanwise averaging. In an actual experiment, it is most likely that both modes(sinuous and varicose) but of unknown relative strength are present. If the contours of varicose and sinuous mode with $-\overline{v'\theta'} > 0$ are arbitrarily superimposed, the resulting contour would strongly resemble $\partial\theta/\partial y$ distribution in the upper boundary layer region[17] of the typical mushroom like structure of θ. The downward transport of heat towards the wall by the eddy heat flux appears on the average over the spanwise direction, as if $-\overline{v'\theta'} \approx \alpha_{eddy}\,\partial\theta/\partial y > 0$ where $\alpha_{eddy} > 0$ is an eddy conduction coefficient. In this conjecture, the temperature gradient near the wall is steepened by the heat transport effect of the secondary instabilities as if in a turbulent flow. It is interesting to note that the transport effects of the heat flux is active in the upper regions of the boundary layer corresponding to the upper dome of $\partial\theta/\partial y$, attributable to the "inviscid" or dynamical part of the shear flow.

The θ mushroom structure is not shown here but is inferable from u distribution of Girgis & Liu[13]. The entire mushroom structure is depressed towards the wall as the secondary instability develops in the streamwise direction (Momayez [8,9]). These contours of developing u'_{rms} give in turn, a picture of developing θ'_{rms} from the extended Reynolds analogy that provides analogies of structural features for $Pr = 1$.

4. Conclusions

Experimental observations of heat transfer enhancement in the presence of Görtler vortices show that the secondary instabilities increase heat transfer much higher than turbulence. This unexpected extra heat transfer is explained, through a theoretical interpretation, by the effect of the secondary instability on the boundary layer in the downwash zones. In fact, secondary instabilities steepen the normal to the wall temperature gradient in this zone and therefore, cause a higher heat transfer capacity.

References cited

1. M. Fiebig, Vortex generators for compact heat exchangers. *J. Enhanc. Heat Transf.* **2**, 43-61, 1995

2. M. Fiebig, Vortices and heat transfer. *Z. Angew. Math. Mech.* **76**, 1-16, 1966

3. G. Delacourt, P. Dupont, H. Peerhossaini, Mesures des transferts thermiques en écoulement de Görtler à nombre de Reynolds modéré., Congrès SFT 2007 Société Française de Thermique (29 mai - 1er juin - les Embiez), 6 page.

4. G. Delacourt,, L. Momayez, P. Dupont, H. Peerhossaini, Des Transferts Thermiques plus Efficaces dans des Couches Limites Laminaires par Rapport a des Couches Limites Turbulentes, Approche Numérique et Expérimentale, 18ème Congres Français de Mécanique, CFM , 2007 Août, 27 -31, Grenoble, France.

5. P. Dupont, L. Momayez, H. Peerhossaini, Domaine d'influence de l'instabilité centrifuge de Görtler sur les transferts thermiques, Congrès Français de Thermique, SFT 2006, Île de Ré, 16-19 mai, 6 page.

6. P. Dupont, L. Momayez, G. Delacourt, H. Peerhossaini, Mesures des transferts de chaleur de Görtler : influence des perturbations amont et contrôle actif potentiel, colloque Groupement de Recherche sur le contrôle du décollement, Paris, Novembre 2005.

7. L. Momayez, P. Dupont, H. Peerhossaini, Effects of vortex organization on heat transfer enhancement by Görtler instability, Int. J. Thermal Sci. **43**, 753-760, 2004.

8. L. Momayez, P. Dupont, H. Peerhossaini, Some unexpected effects of wavelength and perturbation strength on heat transfer enhancement by Görtler instability, Int. J. Heat Mass Transfer **47,** 3783-3795, 2004.

9. L. Momayez, P. Dupont, H. Peerhossaini, Higher heat transfer efficiency in laminar structured boundary layers than in turbulent boundary layers, International Heat Transfer Conference IHTC-13 Sydney. NEW. Australia. 13-18 August 2006

10. J. T. C. Liu, A. S. Sabry, Concentration and heat transfer in nonlinear Görtler vortex flow and the analogy with longitudinal momentum transfer. Proc. R. Soc. A **432**, 1-12. 1991.

11. K. Lee, J. T. C. Liu, On the growth of mushroom like structures in nonlinear spatially developing Görtler vortex flow. Phys. Fluids A **4**, 95-103, 1992.

12. J. T. C Liu, K. Lee, Heat transfer in a strongly nonlinear spatially developing longitudinal vorticity system. Phys. Fluids **7**, 559- 1995

13. Girgis, I. G., and Liu, J. T. C., 2004 Nonlinear Mechanics of Wavy Instability of Steady Longitudinal Vortices and its Effect on Skin Friction Rise in Boundary Layer Flow. Phys. Fluids **18**, 024102 (12 pages), 2006.

14. J. T. C. Liu Heat transfer enhancement by nonlinear wavy instabilities of steady longitudinal vortices in boundary layer flow. Prog. Comput. Heat Mass Transfer, Vol. 1 (R. Bennacer, ed.), Lavoiser, Paris (2005), pp. 190-195.

15. J.T.C. Liu, Nonlinear instability of developing streamwise vortices with applications to boundary layer heat transfer intensification through an extended Reynolds analogy, Phil. Trans. R. Soc. A (submitted 5 Dec. 2007, under review).

16. X. Yu, J. T. C., Liu, The secondary instability in Görtler flow. Phys. Fluids A **3**, 1845-1847, 1991.

17. X. Yu, J. T. C., Liu, On the mechanism of sinuous and varicose modes in three-dimensional viscousiInstability of Görtler rolls. Phys. Fluids **6**, 736-750, 1994.

18. R. Toé, Etude expérimentale de l'instabilité de Görtler : Instabilité secondaire et effets des tourbillons de Görtler sur les phénomènes de transfert thermique. Thèse de doctorat, de l'université de Nantes,1999.J. D.

19. A. Ajakh, Etude expérimentale de l'instabilité de Görtler : identification de critères d'amplification et de l'intermittence; effet de bord d'attaque et forçage de longueur d'onde. Thèse de doctorat de l'université de Nantes, 1997.

20. H. Peerhossaini, J. E. Wesfreid, On the inner structure of streamwise Görtler rolls. Int. J. Heat Fluid Flow **9**, 12-18, 1988.

21. Swearingen, R. F. Blackwelder, The growth and breakdown of streamwise vortices in the presence of a wall. J. Fluid Mech. **182**, 225-290, 1987.